Taylor & Francis
Taylor & Francis Group

Check for updates

Membrane adsorption with polyacrylonitrile prepared with superfine powder-activated carbon, case study: separation process applied in water treatment containing diclofenac

Juliana do Carmo[a], Naiara Mottim Justino[a], Marcelo Seleme Matias[a], Rodrigo Costa Puerari [a], William Gerson Matias [a], David Ladner[b], Denice Schulz Vicentini [a] and Maria Eliza Nagel Hassemer[a]

[a]Department of Environmental and Sanitary Engineering, Technological Center, Federal University of Santa Catarina, Florianópolis, Brazil; [b]Department of Environmental Engineering and Earth Sciences, Clemson University, Anderson, SC, USA

ABSTRACT

Polyacrylonitrile membranes (PAN) have high stability against chemical agents, making them suitable for a wide range of applications as such Ultrafiltration processes. Ultrafiltration membranes composed of PAN/Superfine powder activated carbon (S-PAC) mixtures can be a good research route, aiming the development of a new separation processes for water treatment. The association of materials to form a single product can have technological and economic advantages in separation processes. In this study, S-PAC impregnated into PAN membranes were prepared, characterized and used, as a case study, to remove diclofenac (DCF) from water. The membranes (PAN/S-PAC) were synthesized with different concentrations of S-PAC (0.2, 0.6, 1.0, 3.0 and 5.0 wt%) by a phase inversion process. The results of the TEM characterizations of the S-PAC indicated the presence of micro and nanoparticles (~10 nm) and tending to form micrometric clusters. The infrared spectra of the membranes were characteristic of PAN; however, vibrational bands attributed to the S-PAC spectrum were also observed, which indicated an interaction between the materials. The case study showed an increase in the water flux and in the DCF rejection efficiency, for composite membranes (PAN/S-PAC) with higher concentration of S-PAC. The results of static adsorption tests indicated that the mechanism of DCF rejection occurred predominantly by adsorption. There were indications that the PAN/S-PAC membranes formed a composite material and the PAN/S-PAC (3.0) presented the best study composition given the results. Although the research is in its initial phase, the results indicated that the composition can improve many water treatment systems.
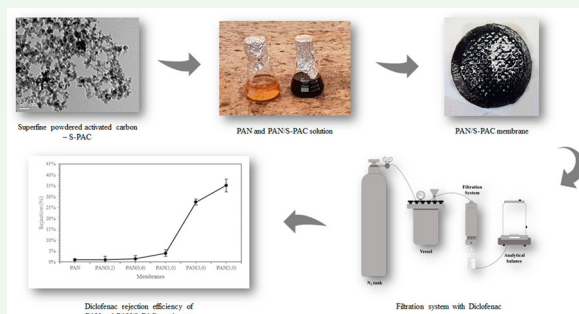
Superfine powdered activated carbon – S-PAC

PAN and PAN/S-PAC solution

PAN/S-PAC membrane

Diclofenac rejection efficiency of PAN and PAN/S-PAC membranes

Filtration system with Diclofenac

1. Introduction

The development of new medicines, pesticides, and chemicals for various industrial and health sectors sometimes neglects their negative impact on the environment. Therefore, the effects of these compounds when released into the environment are poorly known and the findings do not keep pace with the emergence of new products. Endocrine disruptors (EDs) are considered emerging organic pollutants and are represented by several chemical compounds present in medicines, agrochemicals, packaging, and hygiene products. The presence of EDs in the environment, especially in surface waters, is attributed to the improper disposal of untreated wastewater and the discharge of effluents from water and wastewater treatment plants. One of these EDs is the drug diclofenac (DCF), included by The

European Commission in the list of priority hazardous substances [1]. The drug is considered to be persistent and highly stable under conventional treatment plant conditions [2]. Due to its incorrect discharge in the aqueous environmental, DCF was detected by several works at concentrations between 0.015 and 18.74 µg L^{-1} [3–10], in some cases, way high to the 0.1 µg L^{-1} proposed by the Evaluation of Quality Standards of the European community [11]. The most significant entry routes of DCF in the environment are related to the release from conventional wastewater treatment plants due to DCF recalcitrant characteristic [2].

Efficient removal of drugs at water and wastewater treatment plants depends on the technologies applied. Conventional treatment processes are not designed to remove EDs, thus resulting in surface water discharge even when a treatment plant is present [12]. An alternative way to remove DCF from water is by adsorption using activated carbon (AC). AC is the most widely used material for adsorption due to its high specific surface area and a large number of micropores [10,13]. Beyond the high adsorption capacity, AC is easy to operate and can be produced from several carbonaceous materials, such as wood, coconut shell, rice shell, bituminous coal, and petroleum residues [13,14].

AC has been widely used in powder (PAC) or granular (GAC) forms. Since the specific surface area of AC is an important variable in adsorption, in the past years, different technologies have been tested to produce and apply AC in nanoscale. Milling PAC to very small particle sizes results in a nanosize superfine powdered activated carbon (S-PAC) with faster adsorption kinetics and greater micropollutant removal capacity [15–20]. The most challenge using nano-sized materials is to avoid their leaching from the system and become a contaminant. After use, usually PAC is removed by coagulation/flocculation, sedimentation and filtration by granular media or ultrafiltration (UF) membranes [15,16]. However, due to S-PAC small size, the ultrafiltration membrane has low rejection and high fouling propensity to S-PAC, compromising the water flux [15]. Fouling, or the process of solute or particles deposition onto membrane surface, increases the pressure required to move water through the membrane and contribute to more frequent replacement and cleaning of membranes, contributing to the high operation costs [21]. This effect is a problem since it would lead to a constant need for membranes substitution or washing, affecting the costs of the process.

A solution for this problem may be the fixation of S-PAC on the membranes. Nanofiltration and reverse osmosis membranes are widely used for drug removal [22–26]. Additionally, membranes technologies such as pervaporation (PV) and membrane distillation (MD) are also used in the medical industry [27,28]. However, the energy required for the operation of membrane filtration systems may make their use more expensive and less feasible. Ultrafiltration (UF) involves a membrane with a larger pore size than NF, which is primarily aimed at the removal of organic matter and microorganisms, obtaining low drug rejection efficiencies due to its separation mechanism. Thus, the combination of different types of treatment technologies has been promoted to reach efficient removal of micropollutants, such as the association of UF-NF [10], PAC as pre-treatment to UF [9,10], and the production of composites using adsorbents and polymers [29–31]. Moreover, the high adsorption capacity of S-PAC turns it into a great candidate to compose a UF membrane. Additionally, being entrapped in a membrane matrix, S-PAC will not be released in the environment as a contaminant.

Aiming the combination of S-PAC and UF as an alternative for DCF removal, the present work prepared membranes of polyacrylonitrile (PAN) and S-PAC by the phase inversion process, characterized S-PAC and PAN/S-PAC membranes and evaluate the rejection performance of DCF. The S-PAC and the PAN/S-PAC membranes were characterized by physicochemical techniques. Water flux and membrane rejection efficiency tests were performed in dead-end mode using a pilot filtration system. The effects of adding S-PAC on morphology, properties, and performance of the membrane were investigated.

2. Materials and methods

2.1. Materials

S-PAC was produced by wet milling of coconut-shell based PAC for 20 min (Aquacarb 1230C, Siemens) using a MiniCer mill (Netzsch Premier Technologies, Exton, PA, USA). This procedure was performed by the Membrane Science and Technology Laboratory of the Department of Environmental Engineering and Earth Sciences at Clemson University. Polyacrylonitrile (PAN), dimethylformamide (DMF), and diclofenac (DCF) were purchased from Sigma-Aldrich (St. Louis, USA). The molecular weight of DCF is 296.15 g mol^{-1}, its log K_{ow} is 4.51, and its pKa is 4.15. All the experiments were carried out using reverse osmosis (RO) water (Permutation, RO0420).

2.2. Methods

2.2.1. S-PAC characterization
Specific and external surface area and chemical contents of S-PAC were previously reported by Partlan et al. [32].

This S-PAC had a specific surface area of 1047 m^2 g^{-1} and an external surface area of 5.18 m^2 g^{-1}. The carbon, hydrogen, nitrogen, and oxygen contents were 90.9%, 0.05%, 0.03%, and 4.06%, respectively. Size and shape of S-PAC were characterized by transmission electron microscope (TEM) JEM-1011 TEM (JEOL Ltd., Tokyo, Japan, 100 kV). The hydrodynamic diameter (HD) was measured by dynamic light scattering (DLS) using the Zetasizer NanoZS, and the surface charge properties of adsorbents were investigated by zeta potential measurements (ZP) using the PALS technique, with a Nanobrook 90 Plus PALS (Brookhaven, New York, USA). Readings were taken in RO water after bath sonication, and z-avg hydrodynamic diameters are reported. Functional groups on the surface of S-PAC was investigated by Fourier transform infrared spectroscopy using the attenuated total reflectance technique (FTIR-ATR) by an Agilient Cary 600 Series FTIR Spectrometer.

2.2.2. Membrane preparation

PAN membranes were prepared by non-solvent induced phase inversion method. PAN was dissolved in DMF (15 wt%). For PAN/S-PAC composite membranes, S-PAC was added to DMF at different percentages of 0.0, 0.2, 0.6, 1.0, 3.0 and 5.0 wt% which will be referred as PAN (neat membrane), PAN (0.2), PAN(0.6), PAN(1.0), PAN (3.0) and PAN(5.0), respectively. For the preparation of the PAN/S-PAC membrane solution, S-PAC was dispersed in DMF by sonication bath for 60 min to minimize S-PAC aggregation. After S-PAC dispersion in DMF, PAN was added into the DMF/S-PAC suspension, sonicated and kept under constant stirring for 36 h at 40°C. The solution polymer was cast onto a glass plate and spread with a doctor blade casting knife with 2 mm s^{-1} speed and 200 μm thickness. Then, the glass plate was immersed into the coagulation bath of RO water at 20°C. After complete precipitation, the membrane was passed through a second bath to remove the excess solvent and were stored in RO water.

2.2.3. Membrane characterization

2.2.3.1. Scanning electron microscopy with field emission gun (FESEM).
Morphology changes in composite membranes caused by the addition of S-PAC in PAN membrane were investigated using FESEM (JEOL, JSM-6701F). Membranes cross-sections were obtained by an argon ion beam cross-section polisher (JEOL, SM-09010). To avoid charging under the electron beams used during FESEM analysis, all samples were previously coated with a gold layer using a high vacuum sputter-coater (LEICA, EM SCD 500). Membrane thickness and porous size were measured using ImageJ software.

2.2.3.2. Fourier transform infrared spectroscopy using the attenuated total reflectance technique (FTIR-ATR).
The functional groups present on PAN and PAN/S-PAC membranes were determined by FTIR-ATR spectroscopy using an Agilent Cary 600 Series FTIR Spectrometer. The technique is characterized by internal reflection spectroscopy in which the sample is placed in contact with zinc selenide crystal (ZnSe). Samples were carried out in a spectral range of 400–4000 cm^{-1}. Samples were prepared by drying in an oven at 50°C for 24 h.

2.2.3.3. Water content, pore statistics and dimensional stability.
Hydrophilicity property and pore proportion difference of membranes caused by the addition of S-PAC in the polymer matrix were evaluated Water content was measured by comparing the wet and dry weight of membrane samples (2 × 2 cm). First, excess of water was removed of the wet membrane with a paper towel and weigh in precision analytical balance. Then, the samples were dried in an oven at 50 °C for 24 h and then weighed again. The thickness of wet and dry membranes was also measured using a Digimess IP54 digital external micrometer. The water content (W) and the porosity statistic (P) were calculated using the expression given in Equation (1) and Equation (2):

$$W(\%) = \frac{W_{wet} - W_{dry}}{W_{wet}} \times 100 \qquad (1)$$

$$P(\%) = \frac{W_{wet} - W_{dry}}{\rho \times V} \times 100 \qquad (2)$$

where W_{wet} and W_{dry} are the weights (g) of the wet and dry membranes, respectively, ρ is the water density (0.998 g cm^{-3}), and V (cm^3) is the volume of the membrane.

All tests were performed in triplicate.

Another property that may be influenced by the addition of a filler into matrix polymer is the dimensional membrane stability (Dim). Dim consists of the difference between the area of dry and wet membranes and was calculated by the following equation.

$$Dim(\%) = \left(1 - \frac{S_{dry}}{S_{wet}}\right) \times 100 \qquad (3)$$

where S_{wet} and S_{dry} are the area (cm^2) of the wet and dry membranes, respectively. The tests were performed in triplicate with different membrane sample in each repetition.

2.2.4. Water flux measurements

All filtration experiments were performed in a dead-end filtration system coupled with a 5 L stainless steel tank. The system was pressurized by nitrogen gas and the

experiments were carried on at room temperature (~20°C). The membrane effective area was 9.6 cm^2. Membrane compaction was performed by water filtration (RO water) at different transmembrane pressures of 1, 2, 3 and 4 bar. For each pressure, the flux was monitored until stabilization. The permeate volumes were collected during 1 min and weighted in a precision analytical balance. Thus, the water flux was calculated by the following equation.

$$J = \frac{V}{S \times t} \quad (4)$$

where J is the flux of the membrane (L m^{-2} h^{-1}), V is the permeate volume (L), S is the membrane surface area (m^2) and t is the time set for permeate collection (h).

The assays were performed in triplicate with different membrane sample in each repetition.

2.2.5. Diclofenac removal performance

2.2.5.1. Diclofenac filtration.
Subsequently to water flux measurements, the compacted membranes were subjected to the DCF rejection experiment. DCF solution (5 mg L^{-1}) was filtered with a pressure of 2 bar and temperature of 20°C. Aliquots were collected every 5 min. DCF concentration of feed and permeate were determined with a UV-visible spectrometer (Global Trade Technology, GTA-96, range 190–1000 nm). The absorption wavelength of the DCF is in the range of 200–350 nm, exhibiting a maximum at 275 nm. The removal performance was evaluated according to the following equation.

$$R(\%) = \left(1 - \frac{C_p}{C_f}\right).100 \quad (5)$$

where C_P and C_f is the permeate concentration and the feed concentration, respectively.

The tests were performed in triplicate with different membrane sample each time. The pH of the DCF solution was not altered for more precise simulation of an environmental scenario.

2.2.5.2. Static adsorption of DCF.
In order to differ rejection mechanisms of filtration and adsorption, a static adsorption experiment was performed. Membrane samples (1 × 1 cm) were placed into glass flasks with 15 mL, of 5 mg L^{-1} DCF solution. The flasks were put in a shaker table for 2 h. Subsequently, the concentration of DCF in the bottle was determined via UV-visible spectrometry at wavelength of 275 nm and compared to initial absorbance/concentration. The experiment was carried out in triplicate with new membrane sample in each repetition.

3. Results and discussion

3.1. S-PAC characterization

TEM images (Figure 1) show S-PAC particles at micro and nanometric scale. There are dense micrometer domains distributed between the clusters of nanoparticles. The average nanoparticles diameter is 10.25 ± 2.99 nm, while the clusters have a size between 400 and 800 nm. The morphology of the nanoparticles tends to spherical and with tendency to form clusters, while the morphology of the microparticles is irregular and dispersed. These formations are characteristic of milling process. Particles milled for long time result in small, spherical and more homogeneous shape, but particles milled for shorter times are bigger and have more angularity. This indicate that the milling time was insufficient to meet 100% of homogeneous and nano scale particles. As milling time increased, ph of all carbons decreased and the oxygen content of all carbons increased. Oxygen increases also correlated strongly with specific external surface area, which is consistent with the idea that oxidation is happening primarily on the external surfaces [32].

The zeta potential measurement of the S-PAC suspension in RO water resulted in −24.04 ± 1.04 mV, indicating intermediate stability for the S-PAC particles at pH 6.4. This result is not considered stable because there is a borderline between stable and unstable suspensions set at 30 mV and −30 mV [33]. The mean hydrodynamic diameter was 475.08 ± 6.47 nm, which is in accordance with TEM images.

3.2. Morphologies of the membranes

PAN/S-PAC membranes had a uniform colour suggesting a homogeneous distribution of S-PAC within PAN matrix. Figure 2 shows FESEM micrographs of the cross-section of PAN and PAN/S-PAC membranes. All membranes exhibited a typical asymmetric structure of ultrafiltration, composed of a thin skin layer and a finger-like macrovoid sublayer (Figure 2). The surface morphology of membranes was not significantly affected by the increase of S-PAC in the polymer matrix in terms of roughness or presence of nodular structures. The images showed uniform surfaces on the membranes, independent of the amount of S-PAC added. The presence of S-PAC influenced cross-sectional morphology. The macrovoids of the PAN membranes were changed in all membranes, giving rise to irregular forms (Figure 2). These modifications can be attributed to the slow transport of solvent and non-solvent in the membrane preparation when the S-PAC particles were added [34].

Furthermore, the size of the macrovoids was observed to increase with the content of S-PAC, especially in PAN
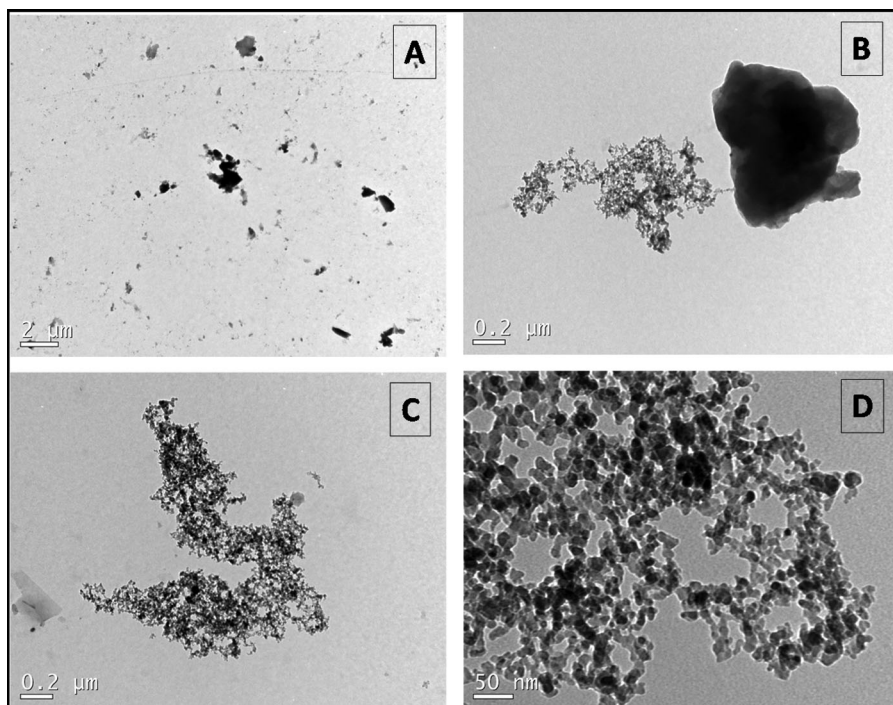
Figure 1. TEM images of the S-PAC particles at different scales (A) 2 µm, (B) and (C) 0.2 µm and (D) 50 nm.

(1.0), PAN(3.0) and PAN(5.0). This may have resulted from the interconnectivity of macrovoids. During phase inversion, the presence of S-PAC may made the connection between polymer chains more difficult, resulting in larger and irregular macrovoids. The presence of S-PAC also shows influence on membrane thickness. The PAN/S-PAC membranes are slightly thicker than pristine membrane which may relate this effect with the increase in viscosity of casting solutions [35] and the consequent influence on solution spread in the plate before coagulation bath. In addition, S-PAC particles can be visualized attach in polymeric matrix in Figure 3 with average size of 0.421 ± 0.135 µm. These particles can be S-PAC microparticles, as identified in TEM images, or aggregates of S-PAC nanoparticles. These clusters may be anchored by the PAN matrix allowing interaction between S-PAC and DCF solution during the filtration process. Apul et al. [29] also found clusters and dispersed S-PAC particles in the polymer matrix when analysing images of polystyrene (PS) fibres with the addition of 5.0% S-PAC.

Micro pore diameter were measure by analysing PAN, PAN(1.0), PAN(3.0) and PAN(5.0) FESEM micrographs (Table 1). The pore size distribution was carried out by analysing the FESEM micrographs in ImageJ and is shown in Supplementary Figure 1. The mean pore size was significant different ($p > .05$) between the samples after applying ANOVA one-way analysis of variance followed by Tukey's post hoc for multiple comparisons. This result indicated that the addition of S-PAC to PAN matrix contributed to an increase of its pores and it is a relevant morphological parameter, directly related to the permeate flux.

3.3. Spectroscopic analysis

Vibrational absorption bands at 2937 cm^{-1} indicated asymmetric axial deformation of the CH$_2$ bond. Bands at 2242 cm^{-1} were related to axial deformation of the nitrile (C≡N). Bands at 1452 cm^{-1} represented asymmetric angular deformations of CH$_2$. Bands at 1248 cm^{-1} represented the CN bonding vibrational axial deformations in amines. This spectrum is typical of polymer materials produced with PAN [35–37]. The vibrational bands observed for PAN/S-PAC membranes were, in general, similar to those found for the PAN membrane (Figure 4); however, it was possible to verify that the region between 2916 and 2838 cm^{-1} presented additional bands characteristic of the S-PAC. These bands are attributed to axial deformation of CH-bonding for aromatics. The vibrational absorption band at 1550 cm^{-1} is characteristic of C = C of aromatics and attributed to the S-PAC.

3.4. Water content, pore statistics and dimensional stability

The hydrophilicity and porosity of the membranes are parameters related to the water flux. As the amount S-PAC
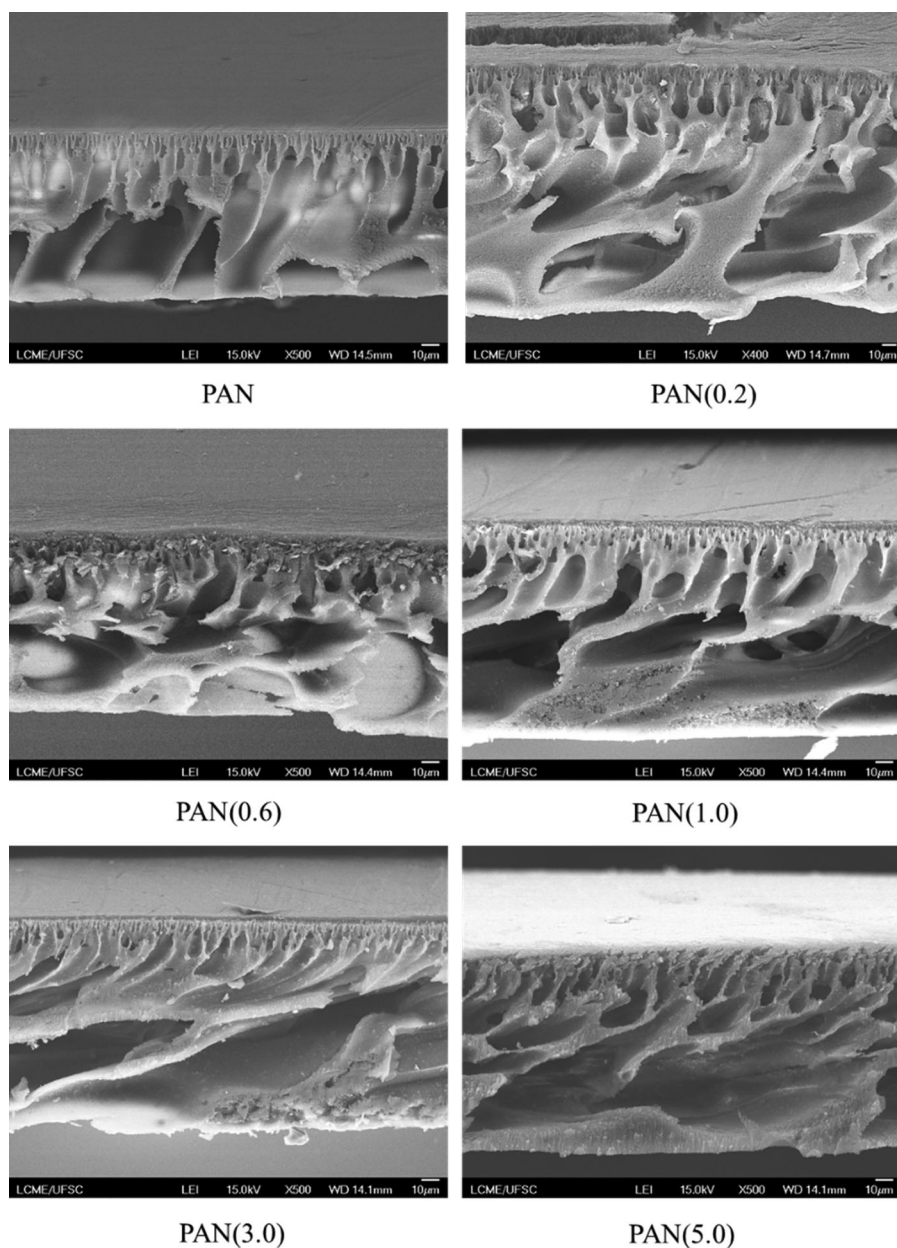
Figure 2. SEM-FEG images of the cross-section of the PAN and PAN/S-PAC membranes. 10 μm Scale.
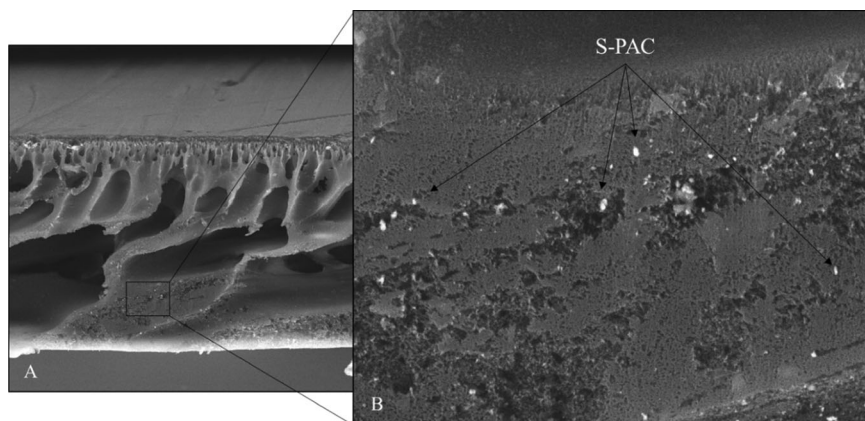

Figure 3. SEM-FEG images of the cross-section of the PAN(1.0). Scale (A) 10 μm and (B) 1 μm. Clusters of S-PAC are visible in panel B.

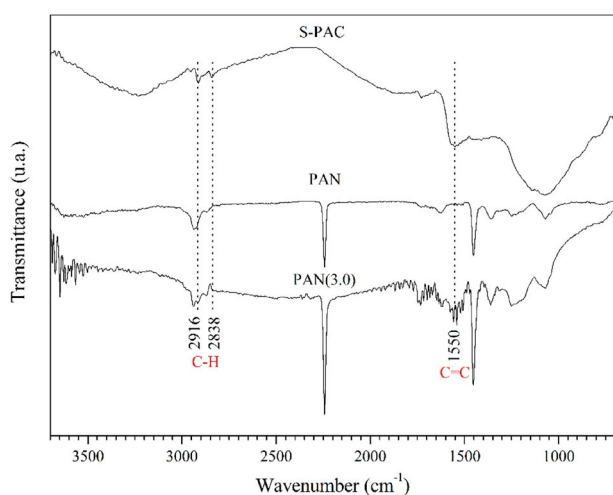**Table 1.** Mean pore diameter of PAN, PAN(1.0), PAN(3.0) and PAN(5.0).

Membranes	Mean pore diameter (μm)
PAN	0.08 ± 0.02^a
PAN(1.0)	0.08 ± 0.03^b
PAN(3.0)	0.10 ± 0.03^c
PAN(5.0)	0.11 ± 0.04^c

Note: The letters [a], [b] and [c] refer to homogeneous groups.

Table 2. Water content and pore statistics of PAN and PAN/S-PAC membranes.

Membranes	Water content (%)	Pore statistics (%)	Dimensional reduction (%)
PAN	84.56 ± 0.02	83.63 ± 2.48	41.17 ± 5.84
PAN(0.2)	85.68 ± 0.11	85.07 ± 1.81	34.67 ± 4.62
PAN(0.6)	85.61 ± 0.03	87.38 ± 2.92	24.83 ± 6.60
PAN(1.0)	85.55 ± 0.36	87.95 ± 5.86	20.50 ± 5.20
PAN(3.0)	86.88 ± 0.57	87.05 ± 4.74	19.00 ± 0.00
PAN(5.0)	87.17 ± 0.53	92.45 ± 0.54	19.00 ± 0.00

increased the water content and pore statistics also saw a small increase compared to the PAN membrane (Table 2). The pore statistics raised from 83.63% for the PAN membrane to 92.45% for the PAN(5.0). However, statistically there is no significant difference between the average porosity values of the evaluated membranes. Thus, although the images provide indications that there was a decrease in solvent and non-solvent exchange kinetics in the phase inversion process, the porosity was maintained with the proportion of CAP-S added.

The water content results showed slight variation among the evaluated membranes. The addition of S-PAC resulted in an increase of water content inside their large macrovoids and also because of the hydrophilic property of S-PAC. The same effect occurred with Gao et al. [34] in the evaluation of the parameter in PAN membranes with carbon porous hollow spheres.

Dimensional stability test of PAN and PAN/S-PAC membranes reveal that as S-PAC was add into PAN the dimensional stability was increased. It means that the incorporation of S-PAC into the membrane reduces its deformation in approximately 50% for PAN(1.0), PAN (3.0) and PAN(5.0) in relation to PAN. Another factor that may have influenced the stability of PAN/S-PAC membranes is the larger macrovoids size of PAN/S-PAC membranes, mostly PAN(1.0), PAN (3.0) and PAN(5.0).

Figure 4. Combined FTIR-ATR spectra of S-PAC, PAN and PAN (3.0).

Larger macrovoids may favour water inlet and outlet motion and thus reducing dimensional changes.

3.5. Flux measurements

The pure water flux of membranes was measured by water filtration until stabilization, at 2 bar. As shown in Figure 5, the water flux of membranes improved with the progressive addition of S-PAC in the PAN matrix. Water permeation was improved by approximately 45% for PAN(5.0) compared to PAN membrane. In general, the pure water flux is determined by the hydrophilicity, porosity and thickness of the membrane [34]. Thus, the flux enhancement of PAN/S-PAC is probably related to their larger pore and macrovoids as S-PAC concentration increased.

Water flux of PAN, PAN(1.0), PAN(3.0) and PAN(5.0) was also measured at different pressures (1, 2, 3 and 4 bar) and is shown in Figure 6. Due to the similarity of PAN(0.2) and PAN(0.6) water flux with PAN and PAN (1.0), respectively, PAN(0.2) and PAN(0.6) were not evaluated. As expected, the water flux increased along with the pressure. However, at 4 bar, the increase flux rate is not so pronounced. The permeability values, obtained by the slope of the straight line through the origin, were 0.067, 0.072, 0.082 and 0.102 m^3 m^{-2} h^{-1} bar^{-1} for PAN, PAN(1.0), PAN(3.0) and PAN(5.0), respectively. The permeability of the membrane can be understood as the measure of the facility that the membrane offers to the passage of a solvent [38]. Thus, it is seen that the permeate flux presented an increasing dependence with the pressure for all the membranes and the permeability improved with the addition of the S-PAC content. In general, an ideal membrane would have high permeability and high selectivity, so this result can be considered positive.

3.6. Diclofenac filtration

The DCF retention efficiency increased with the amount of S-PAC added in the polymer matrix (Figure 7). The highest S-PAC concentrations of PAN(3.0) and PAN(5.0) show significant increase of DCF rejection, 26% and
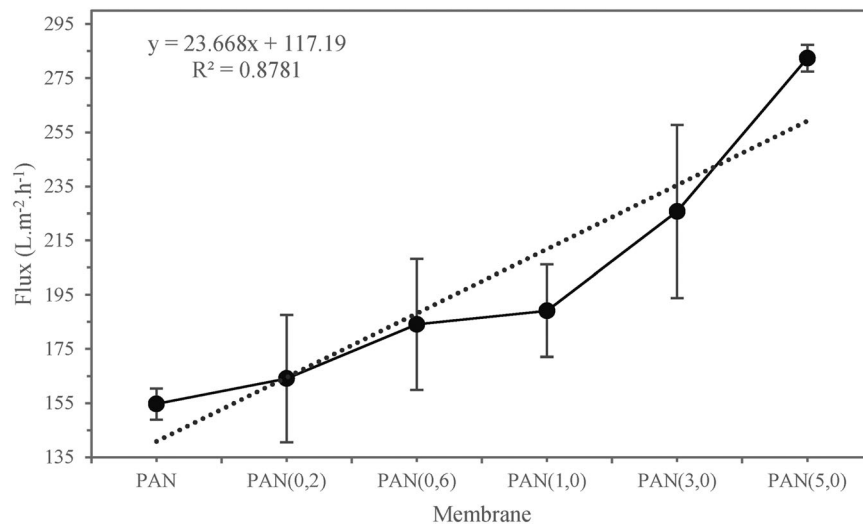
Figure 5. Flux resulting from the PAN and PAN/S-PAC membranes. Pressure at 2 bar.

45% respectively after stabilization. These membranes also present the highest water flux compared to PAN and lower S-PAC loaded, as mentioned before. The highest water flux of PAN(3.0) and PAN(5.0) can be associated with the increase of mean pore size (Table 1) and their greater DCF removal were due the presence of high concentrations of S-PAC. It suggests that the adsorption mechanism of the S-PAC particles was essential for DCF rejection.

Associate high flux and rejection is one of the main challenges in membrane development. UF itself is ineffective for DCF removal (∼10%) because of its high molecular weight cutoff (MWCO) [39]. Testing an hydrophilic commercial polyethersulfone nanofiltration membrane for DCF rejection, Vergili [40] observed rejection of 61% but applying higher pressure (12 bar) and obtaining lower water flux (137 L m^{-2} h^{-1}) compare to our work. This shows how increasing rejection of a high

flux UF membrane can be beneficial in terms water production and energetic costs. S-PAC added in PAN (0.2), PAN (0.3) and PAN (1.0) did not significantly contribute to the DCF rejection. It can be inferred that the small concentration of S-PAC result in almost total encapsulation of the S-PAC by PAN during phase inversion, blocking the penetration of DCF molecules into the active sites of S-PAC [29]. Since the contact between adsorbent and adsorbate is essential to adsorption kinetics, the concentration of S-PAC load must be sufficient to DCF have access to active sites of S-PAC. Following the trend presented in this work, it is possible that adding more S-PAC into PAN matrix could present even higher efficiencies results.

It can also be observed in Figure 7 that all membranes exhibited similar curves of rejection during the experiment, highest at start and decreasing until stabilization
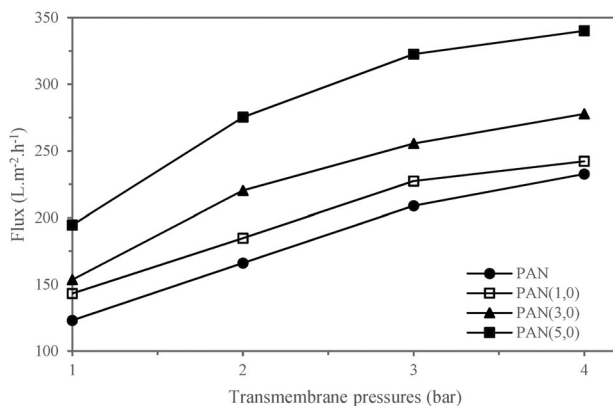

Figure 6. Permeate flux of PAN, PAN(1.0), PAN(3.0) and PAN(5.0) membranes as function of the different transmembrane pressures.
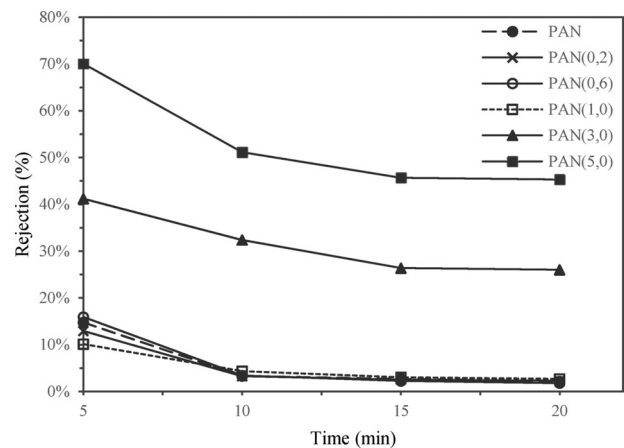

Figure 7. DCF rejection efficiency of the PAN and PAN/S-PAC membranes versus time of the filtration test. Transmembrane pressure at 2 bar. Concentration of feed solution of 5 mg L^{-1}.

Table 3. DCF rejection efficiency and adsorptive capacity of PAN and PAN/S-PAC membranes.

Membranes	Rejection (%)	Adsorptive capacity ($\mu g \, cm^{-2}$)
PAN	1.03 ± 0.39	0.79 ± 0.33
PAN(0.2)	1.10 ± 1.47	0.82 ± 1.08
PAN(0.6)	1.45 ± 1.48	1.09 ± 1.08
PAN(1.0)	4.11 ± 1.56	3.15 ± 1.28
PAN(3.0)	27.55 ± 1.36	20.89 ± 1.93
PAN(5.0)	35.27 ± 2.94	26.78 ± 3.45

at 15 min. This is a common behaviour in the rejection of pollutants by the membrane adsorption mechanism [30,34].

3.7. Static adsorption of DCF

The static adsorption of DCF in PAN and PAN/S-PAC membranes was evaluated after 2 h of interaction between the membranes and the adsorbate solution and are summarized in Table 3. The highest rejection and adsorptive capacity values were concentrated on the PAN(3.0) and PAN(5.0) membranes, corroborating the results of the DCF rejection assay in the filtration process. In addition, PAN, PAN(0.2), PAN(0.6) and PAN (1.0) obtained low DCF retention and small variations among them.

Thus, the results of the static adsorption test indicate that the predominant mechanism of DCF rejection occurs through the adsorption process. By the similarity between the rejection of the 2 h of static adsorption and the fast passage of permeate though membrane by UF, it can be inferred that, in fact, this is the adsorptive capacity of available sites of S-PAC inside PAN.

4. Conclusions

The prepared membranes showed asymmetrical structures and pore size characteristic of ultrafiltration membranes. PAN and S-PAC (micro and nanometric) were compatible in all concentrations loaded into the polymer matrix. The addition of S-PAC modified the morphology of the membranes, leaving them slightly thicker and with larger macrovoids. However, there was no significant change in membrane surfaces. The addition of S-PAC also promoted higher porosity and higher permeability compared to neat membranes. The dominant mechanism of DCF rejection was adsorption by the S-PAC since the PAN membranes presented insignificant results for the DCF removal. Both water flux and DCF rejection increased as the S-PAC concentration increased, being a great trend to be further investigate with higher concentrations of S-PAC. We also recommend assays concerning the fouling proprieties of

these membranes. Overall, these results highlight the possibility of the combination of S-PAC and PAN membranes for water treatment.

Disclosure statement

No potential conflict of interest was reported by the author(s).

ORCID

Rodrigo Costa Puerari http://orcid.org/0000-0003-3858-4905
William Gerson Matias http://orcid.org/0000-0002-2386-0578
Denice Schulz Vicentini http://orcid.org/0000-0001-7080-9911

References

[1] European Commission. Proposal for a DIRECTIVE OF THE EUROPEAN PARLIAMENT AND OF THE COUNCIL amending Directives 2000/60/EC and 2008/105/EC as regards priority substances in the field of water policy, Proposal for a DIRECTIVE. Brussels; 2012.

[2] Ghiselli G. Avaliação da qualdade das águas destinadas ao abastecimento público na região de Campinas: ocorrência e determinação dos interferentes endócrinos (IE) e produtos farmacêuticos e de higiene pessoal (PFHP). Campinas (São Paulo): Universidade Estadual de Campinas; 2006.

[3] Ginebreda A, Muñoz I, López M, et al. Environmental risk assessment of pharmaceuticals in rivers: Relationships between hazard indexes and aquatic macroinvertebrate diversity indexes in the Llobregat River (NE Spain). Environ. Int. 2010;36:153–162. DOI:10.1016/j.envint.2009.10.003.

[4] Hilton MJ, Thomas KV. Determination of selected human pharmaceutical compounds in effluent and surface water samples by high-performance liquid chromatography – electrospray tandem mass spectrometry. J

Chromatogr A. 2003;1015:129–141. DOI:10.1016/S0021-9673(03)01213-5.

[5] Montagner CC, Jardim WF. Spatial and seasonal variations of pharmaceuticals and endocrine disruptors in the Atibaia River, Sao Paulo State (Brazil). J Braz Chem Soc. 2011;22:1452–1462. DOI:10.1590/S0103-50532011000800008.

[6] Rebollo CP, Calvo MG, Villaizán MJLdA, et al. Repercusiones sanitarias de la calidad del agua: Los residuos de medicamentos en el agua. Rev Salud Ambient. 2011;11:17–26.

[7] Roberts PH, Thomas KV. The occurrence of selected pharmaceuticals in wastewater effluent and surface waters of the lower Tyne catchment. Sci Total Environ. 2006;356:143–153. DOI:10.1016/j.scitotenv.2005.04.031.

[8] Sanson AL. Estudo da extração e desenvolvimento de metodologia para determinação simultânea de microcontaminantes orgânicos em água superficial por GC-MS e métodos quimiométricos. Ouro Preto (Minas Gerais): Universidade Federal de Ouro Preto; 2012.

[9] Sheng C, Nnanna AGA, Liu Y, et al. Science of the total environment removal of Trace Pharmaceuticals from water using coagulation and powdered activated carbon as pretreatment to ultra filtration membrane system. Sci. Total Environ. 2016;550:1075–1083. DOI:10.1016/j.scitotenv.2016.01.179.

[10] Vona A, di Martino F, Garcia-Ivars J, et al. Comparison of different removal techniques for selected pharmaceuticals. J Water Process Eng 2015;5:48–57. DOI:10.1016/j.jwpe.2014.12.011.

[11] Hanif H, Waseem A, Kali S, et al. Environmental risk assessment of diclofenac residues in surface waters and wastewater: a hidden global threat to aquatic ecosystem. Environ. Monit. Assess. 2020;192. DOI:10.1007/s10661-020-8151-3.

[12] Petrie B, Barden R, Kasprzyk-hordern B. Sciencedirect A review on emerging contaminants in wastewaters and the environment : Current knowledge, understudied areas and recommendations for future monitoring. Water Res. 2015;72:3–27. DOI:10.1016/j.watres.2014.08.053.

[13] Worch E. Adsorption technology in water treatment. Berlin/Boston: De Gruyter; 2012. https://doi.org/10.1515/9783110240238.

[14] Thomas WJ, Crittenden B. The development of adsorption technology. Adsorpt Technol Des. 1998. DOI:10.1016/B978-075061959-2/50002-1.

[15] Amaral P, Partlan E, Li M, et al. Superfine powdered activated carbon (S-PAC) coatings on microfiltration membranes: effects of milling time on contaminant removal and flux. Water Res. 2016;100:429–438. DOI:10.1016/j.watres.2016.05.034.

[16] Ellerie JR, Apul OG, Karanfil T, et al. Comparing graphene, carbon nanotubes, and superfine powdered activated carbon as adsorptive coating materials for microfiltration membranes. J Hazard Mater. 2013;261:91–98. DOI:10.1016/j.jhazmat.2013.07.009.

[17] Matsui Y, Nakao S, Sakamoto A, et al. Adsorption capacities of activated carbons for geosmin and 2-methylisoborneol vary with activated carbon particle size: effects of adsorbent and adsorbate characteristics. Water Res. 2015;85:95–102. DOI:10.1016/j.watres.2015.08.017.

[18] Matsui Y, Nakao S, Taniguchi T, et al. Geosmin and 2-methylisoborneol removal using superfine powdered activated carbon: shell adsorption and branched-pore kinetic model analysis and optimal particle size. Water Res. 2013;47:2873–2880. DOI:10.1016/j.watres.2013.02.046.

[19] Matsui Y, Ando N, Sasaki H, et al. Branched pore kinetic model analysis of geosmin adsorption on super-powdered activated carbon. Water Res. 2009;43:3095–3103. DOI:10.1016/j.watres.2009.04.014.

[20] Pan L, Matsui Y, Matsushita T, et al. Superiority of wet-milled over dry-milled superfine powdered activated carbon for adsorptive 2-methylisoborneol removal. Water Res. 2016;102:516–523. DOI:10.1016/j.watres.2016.06.062.

[21] Kang Guo-dong, Cao Yi-ming. Development of antifouling reverse osmosis membranes for water treatment: A review. Water Research. 2012;46(3):584–600. DOI:10.1016/j.watres.2011.11.041

[22] Puerari Rodrigo Costa, Gonçalves Renata Amanda, Justino Naiara Mottim, et al. The influence of amine-functionalized SiO$_2$ nanostructures upon nanofiltration membranes. Environmental Nanotechnology, Monitoring & Management. 2020;13:100287. DOI:10.1016/j.enmm.2020.100287.

[23] Dolar D, Vukovic A, Asperger D, et al. Effect of water matrices on removal of veterinary pharmaceuticals by nanofiltration and reverse osmosis membranes. J. Environ. Sci. 2011;23:1299–1307. DOI:10.1016/S1001-0742(10)60545-1.

[24] Yoon Y, Westerhoff P, Snyder SA, et al. Removal of endocrine disrupting compounds and pharmaceuticals by nanofiltration and ultrafiltration membranes. Desalination. 2007;202:16–23. DOI:10.1016/j.desal.2005.12.033.

[25] Yoon Y, Westerhoff P, Snyder SA, et al. Nanofiltration and ultrafiltration of endocrine disrupting compounds, pharmaceuticals and personal care products. J Memb Sci. 2006;270:88–100. DOI:10.1016/j.memsci.2005.06.045.

[26] Radjenović J, Petrović M, Ventura F, et al. Rejection of pharmaceuticals in nanofiltration and reverse osmosis membrane drinking water treatment. Water Res. 2008;42:3601–3610. DOI:10.1016/j.watres.2008.05.020.

[27] Li S, Li P, Si Z, et al. An efficient method allowing for continuous preparation of PDMS/PVDF composite membrane. AIChE J. 2019;65:1–13. DOI:10.1002/aic.16710.

[28] Xue YL, Huang J, Lau CH, et al. Tailoring the molecular structure of crosslinked polymers for pervaporation desalination. Nat Commun. 2020;11. DOI:10.1038/s41467-020-15038-w.

[29] Apul OG, Hoogesteijn von Reitzenstein N, Schoepf J, et al. Superfine powdered activated carbon incorporated into electrospun polystyrene fibers preserve adsorption capacity. Sci. Total Environ. 2017;592:458–464. DOI:10.1016/j.scitotenv.2017.03.126.

[30] Chatterjee S, De S. Adsorptive removal of arsenic from groundwater using a novel high flux polyacrylonitrile (PAN)–laterite mixed matrix ultrafiltration membrane. Environ. Sci. Water Res. Technol. 2015;1:227–243. DOI:10.1039/C4EW00075G.

[31] Wu H, Tang B, Wu P. Novel ultrafiltration membranes prepared from a multi-walled carbon nanotubes/polymer composite. J Memb Sci. 2010;362:374–383. DOI:10.1016/j.memsci.2010.06.064.

[32] Partlan E, Davis K, Ren Y, et al. Effect of bead milling on chemical and physical characteristics of activated carbons pulverized to superfine sizes. Water Res. 2016;89:161–170. DOI:10.1016/j.watres.2015.11.041.

[33] Malvern instruments. Zetasizer nano series user manual. Dep. Biochem. Biophys. Facil., Univ. Chambridge; 2004. p. 54–54. DOI:10.1016/S0294-3506(99)80105-7.

[34] Gao Y, Qiao Y, Yang S. Fabrication of PAN/PHCS adsorptive UF membranes with enhanced performance for dichloro-phenol removal from water. J. Appl. Polym. Sci. 2014;131:1–9. DOI:10.1002/app.40837.

[35] Majeed S, Fierro D, Buhr K, et al. Multi-walled carbon nano-tubes (MWCNTs) mixed polyacrylonitrile (PAN) ultrafiltra-tion membranes. J Memb Sci. 2012;403–404:101–109. DOI:10.1016/j.memsci.2012.02.029.

[36] Su S, Li J, Zhou L, et al. Ultra-thin electro-spun PAN nanofiber membrane for high-efficient inhalable PM$_{2.5}$ particles filtration. J Nano Res. 2017;46:73–81. www.scientific.net/JNanoR.46.73.

[37] Ren Y, Huo T, Qin Y, et al. Preparation of Flame retardant polyacrylonitrile fabric based on sol-gel and layer-by-layerassembly. Materials (Basel). 2018;11:1–14. DOI:10.3390/ma11040483.

[38] Habert AC, Borges CP, Nobrega R. Processos de Separação por Membranas; 2006.

[39] Secondes MFN, Naddeo V, Belgiorno V, et al. Removal of emerging contaminants by simultaneous application of membrane ultrafiltration, activated carbon adsorption, and ultrasound irradiation. J. Hazard. Mater. 2014;264:342–349. DOI:10.1016/j.jhazmat.2013.11.039.

[40] Vergili I. Application of nanofiltration for the removal of carbamazepine, diclofenac and ibuprofen from drinking water sources. J Environ Manage. 2013;127:177–187. DOI:10.1016/j.jenvman.2013.04.036.